

A MAP OF M—42 AND M—43 AT A WAVELENGTH OF 1.94 CM

By M. A. GORDON*

[Manuscript received November 18, 1968]

Summary

A radio map of the Orion A region, made with a beamwidth of $2' \cdot 2$ arc and a pointing accuracy of $11''$ arc r.m.s., resolves the two nebulae, agrees well with optical photographs, and confirms that the emission peak of M—42 lies some $30''$ arc east of the Trapezium.

INTRODUCTION

The Orion nebula has been mapped at 1.9 cm previously by Zisk (1966) and Terzian, Mezger, and Schraml (1968). The contributions of the map reported here stem from the high pointing accuracy of the antenna. For example, these observations confirm the separation between the Trapezium and the centre of radio emission, measured to be $30''$ arc at 408 MHz by the interferometric observations of Mills and Shaver (1968).

APPARATUS AND PROCEDURE

(a) Radio Telescope

The 120 ft parabolic antenna of the Haystack Microwave Facility is enclosed in a radome. The radome protects the reflector surface from the effects of wind, ice, Sun, and thermal gradients and maintains the high precision of the surface. A Univac 490 digital computer drives the antenna and processes data on a time-shared basis.

The azimuth and elevation drives employ shaft-to-digital encoders having an angular quantum of $2'' \cdot 5$ arc. Extensive observations of radio sources of known positions have established an *on-line* correction function for the antenna pointing. Figure 1 shows absolute pointing errors as functions of elevation and azimuth. The r.m.s. error is $11''$ arc. Meeks, Ball, and Hull (1968) have discussed the antenna pointing in detail.

Allen, Barrett, and Crowther (1968) have described the antenna performance. Subsequent to their measurements, the figure of the antenna, and its stability, has been improved by a rigging of the reflective panels of which the surface is composed. Direct optical measurement shows the surface now to have an r.m.s. roughness of approximately 0.50 mm at elevations between 20° and 70° . Radiometric measurements suggest an r.m.s. roughness of 0.76 mm, however, based upon the random roughness theory of Ruze (1952). At 15.5 GHz, the antenna beam has a circular half-power contour of width (HPBW) of $2' \cdot 2$ arc ($0^\circ \cdot 036$) in diameter. The highest sidelobe is 14 dB below the main lobe. Beam efficiency is approximately 0.33. This value includes a loss of 1.6 dB due to scattering by the radome.

* Lincoln Laboratory, Massachusetts Institute of Technology, Lexington, Massachusetts 02173, U.S.A.

(b) *Radiometer*

The radiometer used for these observations is of the tuned radio frequency (TRF) type and consists of a cascade of tunnel diode amplifiers followed by a travelling wave tube amplifier. The 1 GHz passband is split into contiguous 500 MHz bands for detection. The signal in each of these channels is detected by a precision square-law detector synchronously with the phase of the Dicke-switch in the antenna feeder. Allen and Barrett (1967) have shown the radiometer gain to be stable within 1% over a 40 min period. During operation, the injection of noise into the antenna feeder calibrates the radiometer. This calibration increment is established by frequent comparison with a cryogenic reference load positioned in the antenna feeder.

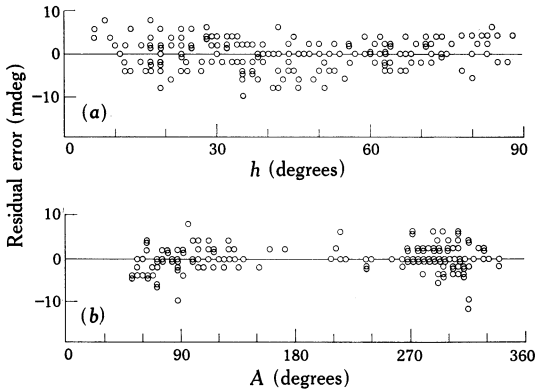


Fig. 1—Pointing errors as a function of:

- (a) elevation h ,
- (b) azimuth A .

(c) *Procedure*

The mapping procedure consisted of making drift scans of the Orion A region. The declination increment was $0^{\circ} \cdot 015$. Each scan was examined for the presence of interference, and if accepted, averaged with others of the same declination. There are approximately three sets of drift scans of each declination position. The data analysis employed computer programmes made available by M. L. Meeks.

The resulting array of drift scan averages was filtered to remove noise of spatial frequencies greater than the antenna's passband. The antenna temperatures of the scans were corrected for an elevation-dependent atmospheric attenuation. Table 1 lists zenith attenuation, due to water vapor and oxygen calculated by the method of Allen and Barrett (1967), for the observation days.

In the mapping procedure, small pointing errors can arise which do not occur during dynamic tracking used to obtain the absolute pointing data of Figure 1. Because of inertia and the viscosity of the hydraulic drive system, the antenna tends to lag slightly behind the digital commands during sidereal tracking. To compensate for this, the servo amplifiers are balanced with electronic biases. During drift scans, however, there is no antenna motion and thus no inertial or viscous forces. Thus, during mapping, these biases cause the antenna position to differ from the command position by several quanta. Although the drift scan data are catalogued by *actual* antenna position so as to compensate for these errors, the size of the error may vary from scan to scan. Consequently, the scan positions cluster near the idealized

command position very nearly in a Gaussian distribution. For this map the half-power width of this Gaussian is $0^{\circ}.003$.

The effect of these errors is to broaden the beamwidth. The broadening may be considered to be a convolution of the Gaussian with the antenna beam. If the antenna beam is considered to be Gaussian of HPBW 36 mdeg, then the effective beamwidth is $\{(3)^2 + (36)^2\}^{\frac{1}{2}}$ mdeg. Thus the broadening is less than 1% and hence negligible.

TABLE I
15.5 GHz ZENITH ATTENUATION IN ATMOSPHERE

Day	Water Vapor (dB)	Oxygen (dB)	Total (dB)
29. xi. 67	0.017	0.064	0.081
30. xi. 67	0.017	0.066	0.083
9. i. 68	0.0018	0.087	0.089
11. i. 68	0.0045	0.077	0.082
12. i. 68	0.0047	0.077	0.082

The scatter of the calibration data of Figure 1 is not wholly systematic; some portion is due to random fluctuations in pointing response. The averaging of many drift scans, as is done here, reduces the effective pointing error. Thus the accuracy of map positions exceeds that of the absolute calibration data.

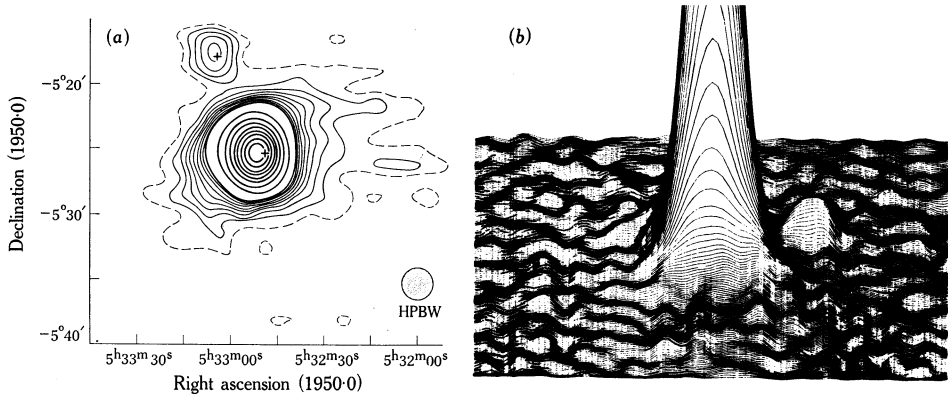


Fig. 2.—A 15.5 GHz map of the radio source Orion A is shown in (a). The inner heavy lines indicate 1 degK contours in antenna temperature, while the thinner lines are 0.1 degK contours. The dashed contours lie 0.1 degK above the r.m.s. noise threshold of the background. The + symbols indicate the positions of the exciting stars.

A ruled surface presentation of the data in (a) as viewed from the west (position angle 270°) is shown in (b). The undulations are background noise. The peak emission from M-42 is not shown.

OBSERVATIONS

Figure 2(a) shows the contour map of the Orion A region, while Figure 2(b) shows a ruled surface display by which the relative amplitude of the background noise fluctuations can be estimated. The nebulae M-42 and M-43 are clearly

separated just as they are in the $\lambda 5200$ photograph by Wurm and Rosino (1959, see Fig. 2 of Gordon and Meeks 1968). Thus the dark lane separating the two nebulae is not due to dust, but represents an actual decrease in the emission. The outline is irregular and consistent with the optical shapes of the nebulae, considering the angular resolution of the radio data.

The half-power contour of M—42 is elliptical, having a major axis of $3' \cdot 4$ arc and a minor axis of $2' \cdot 6$ arc after correction for beam broadening, and a position angle of 10° . The major axis may be perpendicular to the position angle of the spin axis of M—42 (Mezger and Ellis 1968). The half-power contour of M—43 is irregular, with an approximate diameter of $3' \cdot 1$ arc. Table 2 lists the coordinates of the M—42 and M—43 emission peaks and of their probable exciting stars BD— $5^\circ 1325$ and BD— $5^\circ 1315$ (the Trapezium).

TABLE 2
POSITIONS OF STARS AND RADIO MAP CENTRES

Object	Right Ascension (1950.0)			Declination (1950.0)		
	h	m	s	°	'	"
M—42	5	32	$51 \cdot 1 \pm 0 \cdot 7$	—5	25	16 ± 11
BD— $5^\circ 1315$	5	32	48.995	—5	25	$16 \cdot 22$
M—43	5	33	$4 \cdot 5 \pm 0 \cdot 7$	—5	17	34 ± 20
BD— $5^\circ 1325$	5	33	3.747	—5	17	$54 \cdot 89$

The computer calculates the integral of antenna temperature over the region. To relate this quantity to units of emission flux density independent of the antenna system, a similar map of the radio source Virgo A has been made with the same instrumental configuration used for the Orion A observations. If the Virgo A flux density is taken to be $28 \cdot 8 \pm 1 \cdot 8$ f.u.* as suggested by Allen (1967), the flux density of M—42 becomes 357 ± 20 f.u. and of M—43, 8 ± 1 f.u. (The r.m.s. error is an estimated one based upon noise fluctuations, such as those shown in Figure 2(b), for both maps.) The M—42 value agrees with that reported at 14.5 GHz by Baars, Mezger, and Wendker (1965) but is less than the value of 390 f.u. reported at 15.4 GHz by Terzian, Mezger, and Schraml (1968).

The continuum map of Figure 2(a) is the cross-correlation of the true brightness distribution (at 15.5 GHz) with the antenna beam. The beam constitutes a low pass filter which transmits spatial frequencies of the source distribution up to a cutoff determined by the dimensions of the antenna. Within the passband, transmission varies as a function of frequency, and thus the spatial frequencies of Figure 1 have different relative amplitudes than those of the true source distribution. The process of correcting transmitted frequencies for the passband shape is known as "restoration".

In practice it is impossible to effect a perfect restoration. Frequency components exceeding the antenna cutoff are not recoverable, and hence the restored distribution is not, in general, a replica of the true source distribution. Furthermore, the observing process introduces noise. The transmission of the antenna passband decreases

* 1 flux unit = 10^{-26} W m⁻² Hz⁻¹.

towards the cutoff, and hence the signal-to-noise ratio of the observed spatial frequencies decreases in the same sense. Thus restoration is most likely to be accurate for sources with substantial low frequency components, i.e. sources of angular extent large compared with the HPBW.

Bracewell (1955) has discussed restoration techniques which consider the variation of signal-to-noise within the antenna passband. These techniques effect only *partial* restoration in that restoration tends to be confined to low spatial frequencies where signal-to-noise ratios are greatest. He shows one simple method, known as the chord technique, to be as effective as the more mathematically straightforward but operationally complicated process of three successive iterations. Figure 3 shows the brightness distribution along a line joining the centres of M-42 and M-43, calculated by means of a two-dimensional chord technique. The beam efficiency was taken to be 0.33, a value calculated from maps of the radio source Virgo A.

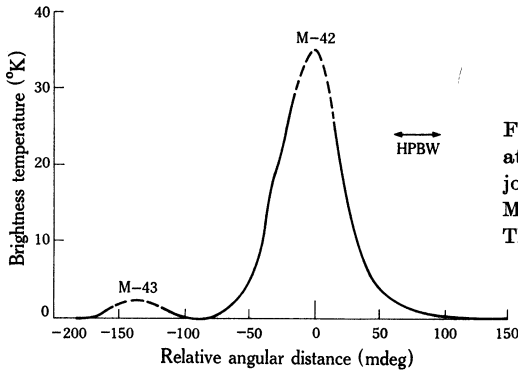


Fig. 3.—Brightness temperature at 15.5 GHz along the line joining the emission peaks of M-42 and M-43. The position angle is 14°.

It is important to remember that chord restoration is only partial. Its effectiveness is greatest for source distributions of predominantly low spatial frequencies. For example, M-42 is optically thick at low wave frequencies, and hence the source distribution should be nearly flat topped. At 15.5 GHz, M-42 is optically thin; the source distribution is more peaked and contains comparatively greater components of high spatial frequency. Thus the 15.5 GHz data are more difficult to restore than low frequency data taken with a similar HPBW. The brightness temperatures within $\pm 1'$ arc of the peaks of M-42 and M-43 may be underestimated, and the curve in Figure 3 is broken at these sections. The bulge on the M-43 side of M-42 is also evident in Figure 2(a) and may correspond to the high velocity component observed by Gordon and Meeks (1968) by means of recombination lines.

Mezger and Henderson (1967) have published an expression for the optical depth τ_ν of an HII region, in the radio range, as a function of frequency ν (GHz):

$$\tau_\nu = 8.235 \times 10^{-2} a T_e^{-1.35} \nu^{-2.1} E, \quad (1)$$

where the variables T_e (°K) and E (pc cm⁻⁶) refer to electron temperature and emission measure respectively. The factor a varies by less than 5% over the frequency and temperature ranges of interest and is taken to be constant here. From equation (1)

$$\tau_{0.408} = 2077 \tau_{15.5}. \quad (2)$$

The brightness temperature T_ν is related to the electron temperature and optical depth by

$$T_\nu = T_e \{1 - \exp(-\tau_\nu)\}. \quad (3)$$

Thus from equations (1) and (3)

$$T_{0.408}/T_{15.5} = \{1 - \exp(-2077 \tau_{15.5})\} / \{1 - \exp(-\tau_{15.5})\}, \quad (4)$$

provided that emission is caused by free-free transitions of the ionized gas and not by other mechanisms.

Substitution into equation (4) of the brightness temperatures specifically quoted by Mills and Shaver (1968) and reported here gives $\tau_{15.5}$ for the centre of M-42. From the optical depths and equation (3), the electron temperature was calculated, and this value and equation (1) were used to evaluate the emission measure. The resulting mean isothermal conditions at M-42 are given below, where the quoted errors are r.m.s.

$T_{15.5}$ (°K)	$T_{0.408}/T_{15.5}$	$\tau_{15.5} \times 10^3$	$\tau_{0.408}$	T_e (°K)	E (10^6 pc cm $^{-6}$)
36 ± 2	217 ± 37	4.6 ± 0.7	10.0 ± 1.5	7600 ± 800	3.1 ± 0.6

DISCUSSION

Mills and Shaver (1968) have mapped the same region at 408 MHz, with approximately the same angular resolution. At this frequency both nebulae are optically thick and hence the shape of their brightness distributions should differ from that observed at 15.5 GHz. Subject to this restriction and the lesser signal-to-noise ratio of the high frequency data, both maps agree well in detail. For example, the weak source located to the west of the Trapezium is evident in both maps.

The similar angular resolution of both maps may suggest that their features may be compared quantitatively. However, the small size of M-43 with respect to angular resolution makes an accurate determination of its central brightness temperature difficult at either frequency. Furthermore, the brightness distribution of M-42 is peaked at 15.5 GHz and flat topped at 408 MHz owing to the great differences in optical depth. Thus, partial restoration is more uncertain for the 15.5 GHz data than for the 408 MHz data for reasons discussed in the previous section. In fact, Mills and Shaver (1968) argue the reliability of their chord restoration of M-42 on the basis of the nearly flat-topped distribution. Therefore, the present paper will compare only brightness temperatures for the centre of M-42 with allowance for the uncertainty of the 15.5 GHz value and the approximation that the gas is isothermal along the line of sight.

Figure 2(a) shows M-42 to have substantial departures from circular symmetry as evident in optical photographs. Such asymmetries probably also exist along the line of sight. Therefore, the conversion of approximate values of E into electron densities is a highly uncertain procedure, and is not attempted here.

The great optical depth of the centre of M-42 at 408 MHz, shown above, had been noted by Mills and Shaver (1968). On that basis, they calculated an electron temperature of 7600 ± 800 °K for the centre of M-42 and noted that the method is

a direct temperature measurement and involves no assumptions regarding the thermodynamic equilibrium of the region. However, the great optical depth also ensures that their measurements refer to the outer regions of the nebula and not to its centre.

The small optical depth requires the 15.5 GHz data to be a mean for conditions through the nebula. Comparison of 15.5 GHz observations to 408 MHz observations is essentially the comparison of data from two different regions of the nebula.

Hjellming (1966) and Sofia (1967) theoretically predict that the electron temperature will vary within an HII region. The exact nature of this variation is a strong function of the spectral type of the exciting star. For the most part, each predicts a general increase in electron temperature as a function of distance from the central star. If this were the case in M-42, then Mills and Shaver's value of $7600 \pm 800^\circ\text{K}$ exceeds the *central* temperature, and the calculated emission measure is too large. In any case, the isothermal approximation would not be a valid one.

Mezger and Ellis (1968) report observations of the 109α recombination line of hydrogen at many points over M-42. Temperatures derived from these measurements suggest an increase in electron temperature away from the centre of the nebula. However, Palmer (1968) shows that the Orion nebula is substantially out of local thermodynamic equilibrium at this frequency, and thus these temperatures are incorrect to some extent (Goldberg 1966) and the apparent temperature variation may be fictitious.

Terzian, Mezger, and Schraml (1968) have also used continuum observations to establish an electron temperature for M-42. Their technique was to extrapolate the M-42 flux density, as a function of frequency, from their observations at 15.4 GHz. These calculations refer to flux densities integrated over the source and assume the source to be isothermal. Each extrapolation requires a tentative electron temperature, and thus they report a value of $3000_{-1000}^{+2000}\text{K}$ gives best agreement between extrapolation and observations. Agreement is most sensitive to observations below 408 MHz and thus to outer regions of the nebula. Comparing their value with the $7600 \pm 800^\circ\text{K}$ of Mills and Shaver (1968), they deduce a temperature decrease away from the centre of M-42. Such a gradient is opposite to that predicted theoretically.

Shaver (1968) has stated that such an electron temperature is erroneously low by a factor of two or more owing to the use of an unrestored brightness temperature distribution at 15.4 GHz. Presumably his argument would be the following. The use of an antenna beam of finite dimensions broadens and smooths the true spatial distribution of brightness temperature. At 15.4 GHz, broadening is especially important because the source distribution is probably not flat topped as it is at low frequencies where $\tau_\nu \gg 1$. Terzian, Mezger, and Schraml in essence derived emission measures for a number of electron temperatures from this broadened distribution. From these, they predicted the total flux density of the source as a function of frequency. The error in electron temperature appears because the emission measures, referring to the broadened distribution, enter *exponentially* into the calculation of brightness temperatures by means of equations (1) and (3), and thus into the predicted flux densities. The effect of the error is to overestimate the flux density contributions from the outer edges of the distribution at low frequencies. At such

frequencies, the great optical depth of the central region of the distribution limits the flux density contribution and no negative compensation occurs from there to offset the edge contributions. Consequently at any given electron temperature the extrapolated *total* flux density of the nebula is too high at low frequencies. A best fit to observations is obtained by means of an erroneously low electron temperature. The magnitude of the error is a function of the source size in terms of the antenna beamwidth.

The problem of determining the electron temperatures of HII regions is a difficult one. Although the comparison of continuum observations in the radio range is a method that is insensitive to departures from thermodynamic equilibrium, the existence of temperature gradients within the nebula may preclude its usefulness. The comparison of the 15.5 and the 408 MHz data led only to limits because the data involved two different locations in the nebula. Observations at one frequency where τ_ν is slightly less than unity and at another where $\tau_\nu \ll 1$ would at least involve the same locations of an HII region. However, this method requires observations of extreme precision to determine electron temperatures of only modest accuracy, owing to the small temperature dependence of the ratio of brightness temperatures. It seems that the best hope of determining a mean electron temperature along the line of sight lies in observations, where $\tau_\nu \ll 1$, of two recombination lines having a common quantum state. This method, proposed by Palmer (1967), has yet to be implemented. Even then, many measurements over the apparent extent of the nebula, as well as assumptions as to its extent along the line of sight, would be required to account for temperature gradients.

A more tangible result of the 15.5 GHz map is the confirmation of the angular displacement between the peak of the radio map of M-42 and the Trapezium, an effect first noted by Mills and Shaver at 408 MHz. As can be seen in Figure 2(a) and Table 2, the Trapezium appears to lie 32" arc to the west of the peak emission of M-42. This distance is approximately three times the r.m.s. pointing error. The Trapezium is the only star cluster in the region which could have produced M-42. The detection of this displacement at a frequency at which M-42 is optically thin means that the central nebula concentration, rather than a surface feature, is not centered at the position of its exciting star cluster.

Menon (1967) calculated an approximate age of 10^5 years for M-42 on the assumption of a uniform motion of the star cluster with respect to the nebula and of an approximate nebula diameter of 1 pc. This age, together with the observed displacement of 32" arc, implies a horizontal velocity component of 1 km sec⁻¹ if the centre of M-42 is taken to be 500 pc from Earth. Observations of hydrogen recombination spectra show M-42 to be moving at approximately 12 km sec⁻¹, with respect to the Trapezium, along the line of sight.

ACKNOWLEDGMENTS

The author gratefully acknowledges discussions with Dr. M. L. Meeks, Dr. S. H. Zisk, and Dr. Yervant Terzian. He is also grateful to the referee who suggested consideration of resolution effects in detail. The Lincoln Laboratory is supported by the U.S. Air Force.

REFERENCES

- ALLEN, R. J. (1967).—Ph. D. dissertation, Massachusetts Institute of Technology (unpublished).
- ALLEN, R. J., and BARRETT, A. H. (1967).—*Astrophys. J.* **149**, 1.
- ALLEN, R. J., BARRETT, A. H., and CROWTHER, P. P. (1968).—*Astrophys. J.* **151**, 43.
- BAARS, J. W. M., MEZGER, P. G., and WENDKER, H. (1965).—*Z. Astrophys.* **61**, 134.
- BRACEWELL, R. N. (1955).—*Aust. J. Phys.* **8**, 200.
- GOLDBERG, L. (1966).—*Astrophys. J.* **144**, 1225.
- GORDON, M. A., and MEEKS, M. L. (1968).—*Astrophys. J.* **152**, 417.
- HJELLMING, R. M. (1966).—*Astrophys. J.* **143**, 420.
- MEEKS, M. L., BALL, J. A., and HULL, A. B. (1968).—The pointing calibration of the Haystack antenna. *IEEE Trans. Antennas Propag.* (in press).
- MENON, T. K. (1967).—I.A.U. Symp. No. 31, p. 121.
- MEZGER, P., and ELLIS, S. A. (1968).—*Astrophys. Lett.* **1**, 159.
- MEZGER, P. G., and HENDERSON, A. P. (1967).—*Astrophys. J.* **147**, 471.
- MILLS, B. Y., and SHAVER, P. A. (1968).—*Aust. J. Phys.* **21**, 95.
- PALMER, P. (1967).—*Astrophys. J.* **149**, 715.
- PALMER, P. (1968).—Ph.D. dissertation, Harvard University (unpublished).
- RUZE, J. (1952).—*Supplto nuovo Cim.* **9**, 364.
- SHAVER, P. A. (1968).—Cornell-Sydney University Astronomy Centre Rep. No. 111.
- SOFIA, S. (1967).—*Annls Astrophys.* **30**, 377.
- TERZIAN, Y., MEZGER, P. G., and SCHRAML, J. (1968).—*Astrophys. Lett.* **1**, 153.
- ZISK, S. H. (1966).—*Science* **153**, 1107.

